

Reconfigurable Cross Dipole - Hash Frequency Selective Surface

M. R. T. de Oliveira¹, M. T. de Melo¹, I. Llamas-Garro², A. G. Neto³

¹Departamento de Eletrônica e Sistemas, Universidade Federal de Pernambuco, Recife, Brazil

²Centre Tecnològic de Telecomunicacions de Catalunya, Castelldefels, Barcelona, Spain

³Instituto Federal de Educação, Ciência e Tecnologia da Paraíba, João Pessoa, Brazil

Abstract: The authors present an RFSS structure with two states based on the cross dipole element. The structure is designed to behave as an array of cross dipole elements in one state, and as an array of hash elements in the other state. The cross dipole patch array has a stop-band filter response, and the hash array behaves as a pass band filter at the design frequency of 12.5 GHz. The frequency response of these filters is analysed using the equivalent circuit method. CST software simulations and experimental results are used to validate the RFSS design.

1. Introduction

One of the devices that has been drawing attention from the scientific community are the Frequency Selective Surfaces (FSS) due to frequency filtering properties. These features make the FSS appropriate for a number of applications from the microwave oven to space vehicles. It's low manufacturing cost, low weight and the possibility of integration with other circuits, favours the development of communications equipment more adapted to market needs.

As an extension of these FSS, one has the reconfigurable FSS (RFSS). While passive FSS have their frequency characteristics invariable, the RFSS has its properties, such as resonance frequency and polarization, varying during its operation. This variation is due to the inclusion of active elements in the structure. One of the active elements used in microwave reconfigurable structures is the PIN diode. When the state of the diode changes from on to off, the properties of the FSS change. The diodes change the FSS response according to an external DC bias source.

Historically, the understanding of the physical principles of FSS evolved directly from the investigation of optical diffraction gratings that are used to decompose a monochromatic light beam in its spectral orders. This decomposition process was discovered by the American physicist David Rittenhouse, as documented in an exchange of letters between him and Francis Hopkinson published in 1786 [1]. Rittenhouse noted the decomposition of white light into different wavelengths which spectral distance depends on the space between the optical diffractive grating wires. The decomposition of white light through a prism has been discovered by Isaac Newton in 1671, but this was the first documented proof that non-continuous surfaces can exhibit different transmission properties for different frequencies of the incident wave [2]. Because of the structure decomposition process simplicity, the concept has been

extended to many areas of science and engineering. Relevant RFSS available in the literature are reviewed below:

An active FSS incorporating PIN diodes as switches is presented in [3]. The unit cell consists of two square loop segments connected by PIN diodes. The frequency response of the surface can be electronically switched from a structure quite transparent to the incident signal with a small insertion loss, to a structure that reflects the incident signal. A tuned multiband FSS is presented in [4]. The unit cell of this structure includes a circular loop slot element on the top side of the substrate and a cross dipole patch on the bottom side of the substrate. The tuning is due to the presence of varactors on both sides of the structure. By changing the capacitances of the varactors, two of the three frequencies of resonance can be displaced. An active FSS for applications in 2.45 GHz is presented in [5]. It consists of circular loop, slot type element with four diodes. The negative bias is provided by the cross dipole, while the positive bias is provided by the circular loop.

This paper proposes a design for RFSS. The unit cell only consists of four cross dipoles that can be connected by four PIN diodes. All unit cells are separated from each other. When the diodes are in the off-state, the four cross dipoles are separated electrically, forming an array of cross dipoles. When the diodes are in on-state, the united four cross dipoles form a hash. The cross dipole has a stop band frequency response, in other words, at the resonant frequency, the FSS will reflect the incident wave. The hash has a pass band frequency response at the designed frequency range, thus the incident wave will propagate through the structure. Therefore, the RFSS has the characteristics of the cross dipole and the hash by simply changing the state of the PIN diode, both with dual TE/TM polarization for an orthogonal incident angle. The novelty of this work is the proposed reconfigurable design between band pass and band stop responses as one moves from hash state to cross dipole state. This feature finds its application in adaptive and RFID antennas.

2. Theoretical basis of Frequency Selective Surfaces

Frequency selective surfaces (FSS), as shown in Fig. 1, can be described as an infinite two-dimensional periodic array, where d is the dielectric thickness, p is the periodicity and g is the space between the elements [6]. These surfaces comprise periodical patch elements with capacitive effect, or slot elements with inductive effect, which respectively show reflection characteristics (patch) or transmission (slot) in the neighbourhood of the resonant element [7], (see Fig. 2). The shape of the elements is not limited to patches or slots, and may be a combination of both. The FSS with slot elements works as a bandpass filter, i.e. at the resonance frequency, the structure becomes a few transparent. On the other hand, the FSS with patch elements acts as a band-stop filter, i.e. at the resonance frequency, the structure

behaves as a perfect conductor, reflecting the incident wave [7]. At wave incidence on the structure, small losses will occur due to dielectric and conductive losses [6]. The resonant frequency depends on the dielectric properties, geometry and element spacing [8]. The understanding of these parameters is essential to have a good FSS design with less computational interactions.

Various geometries can be used to form an FSS element. Munk [9] classifies the elements into four groups. Group 1 comprises poles connected by the centre, such as the dipole, cross dipole, tripole and Jerusalem cross. They resonate when its electrical length is half the wavelength [10]. Group 2 comprises loop type elements such as the circular, square and hexagonal loops. The resonance occurs when the electrical length of each half-loop is a multiple of a half wavelength. Group 3 comprises solid interior or plate type elements with various shapes. Group 4 comprises combinations of elements from groups 1, 2 and 3.

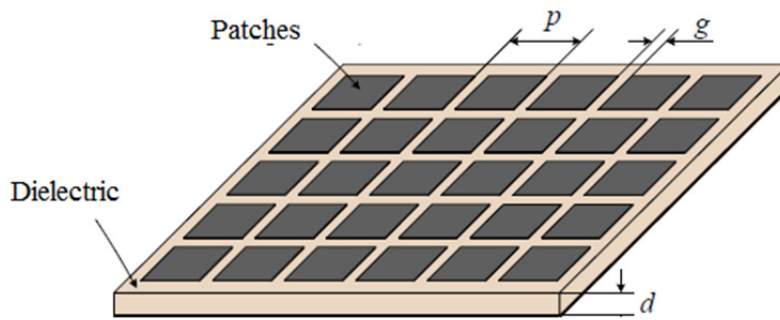


Fig. 1. Two-dimensional periodic structure

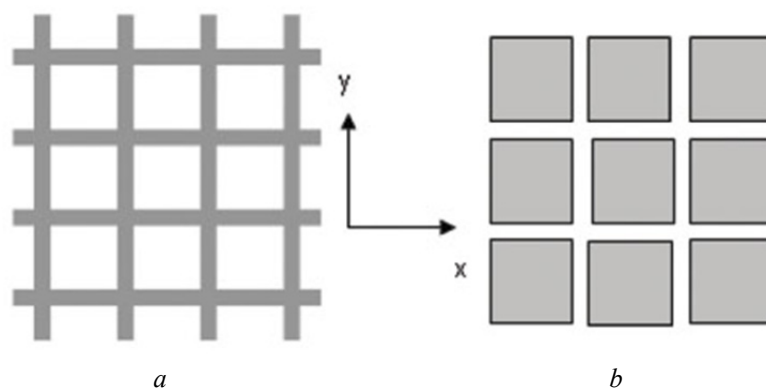


Fig. 2. Element types
a Slot element
b Patch element

3. RFSS Cross Dipole / Hash

A cross dipole is shown in Fig. 3 (a). The cross dipole resonates when its length is a half wavelength. The hash is formed by the union of four cross dipoles, shown in Fig. 3 (b). The hash length is twice the length of the cross dipole, thus its resonance frequency is half of the cross dipole resonance.

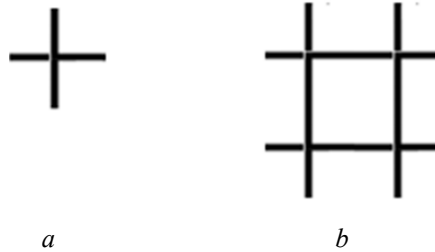


Fig. 3. Elements
a Cross dipole
b Hash

Assuming PIN diodes connect four cross dipoles, when the diodes are in the off-state, the four cross dipoles are separated electrically, forming an array of cross dipoles. When the diodes are in the on-state, the united four cross dipoles form the hash of Fig. 3 (b).

The cross dipole shown here has a stop band frequency response, in other words, at the resonant frequency, the FSS will reflect the incident wave. The hash has a pass band frequency response characteristic at the designed frequency range.

Therefore, the RFSS has the characteristics of the cross dipole and the hash by simply changing the state of the PIN diode. For concept demonstration purposes, the diode will be replaced by a conducting printed strip on the substrate connecting the cross dipoles in the case of the diode on-state, and a spacing between the cross dipoles will be used for the diode off-state. For a more reliable simulation, the PIN diode is modelled as an equivalent circuit which values are extracted from the datasheet MA4AGP907 - Macom.

4. FSS Analysis by Equivalent Circuit Method

The transmission properties of the FSS are estimated by the Equivalent Circuit Method (ECM) [11]. This method is simple and can be used to accurately estimate the resonance frequency of the structures. This technique is based on the comparison between the actual structure and a discrete element LC circuit. The ECM is attractive for presenting a fast, simple and intuitive analysis of the physical mechanisms of the FSS.

The ECM is divided in two parts. The first part of the method aims to find the LC parameters of the equivalent circuit of the FSS. The discrete circuit models for the two states are shown in Fig. 4.

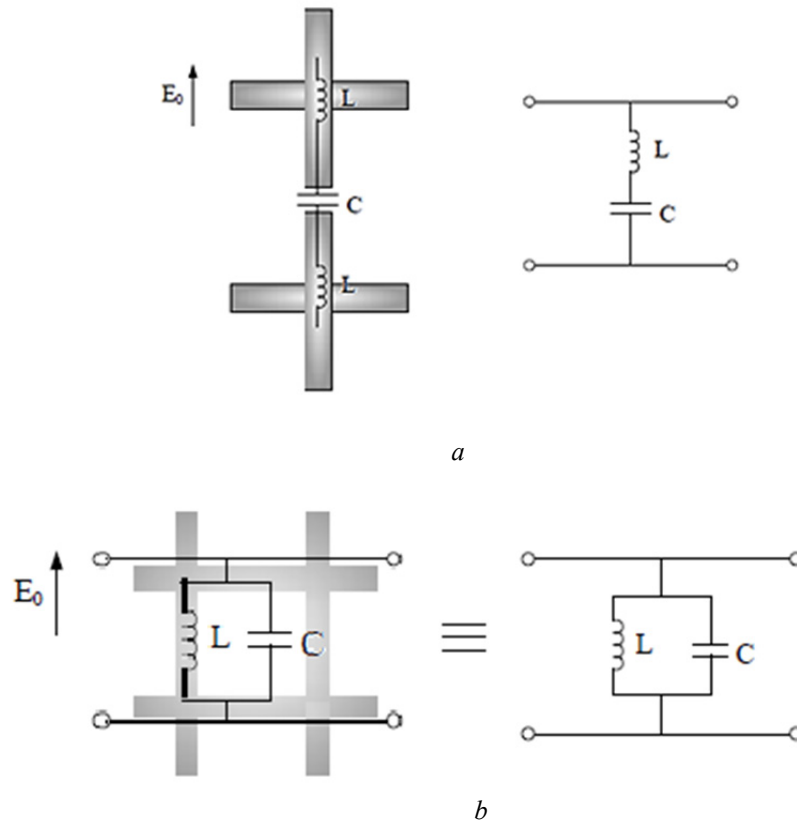


Fig. 4. RFSS unit cell and its respective circuit model
a Cross dipole
b Hash

For simplicity, these models represent the FSS without dielectric (freestanding) and for normal incidence. The second part of the method uses the LC parameters found previously and through simple relationships finds the response of the FSS for various parameters such as structure thickness, dielectric substrate, periodicity and different angles of incidence. The data from the first part of the method is obtained using a full-wave simulation stored in a database. In the second part of the method, the discrete parameters that are in the database can be used to calculate the new parameters of generic configurations using simple calculations. In Fig. 5, the flowchart shows how to design and analyse an FSS structure based on the cross dipole structure.

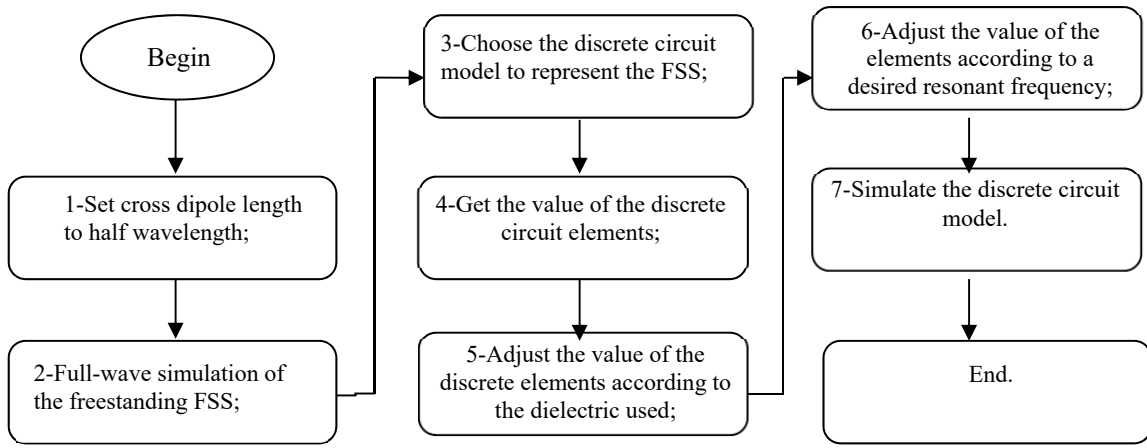


Fig. 5. Flowchart of the equivalent circuit method modelling

5. Design of the RFSS Cross Dipole / Hash

The chosen centre frequency for the RFSS design is $f_0=12.5$ GHz. Following step 1 of the flowchart in Fig. 5, the cross dipole length is set to half wavelength:

$$L_{Dipole} = \frac{\lambda_0}{2} = \frac{c}{2f_0} = 12mm \quad (1)$$

Structure dimensions $L_{substrate}$, W_{dipole} and L_{diode} are shown in fig. 6, values are provided in Table 1 (for step 1 in Fig. 5). The hash, uses a printed conductive tape to short circuit and unite the four cross dipoles.

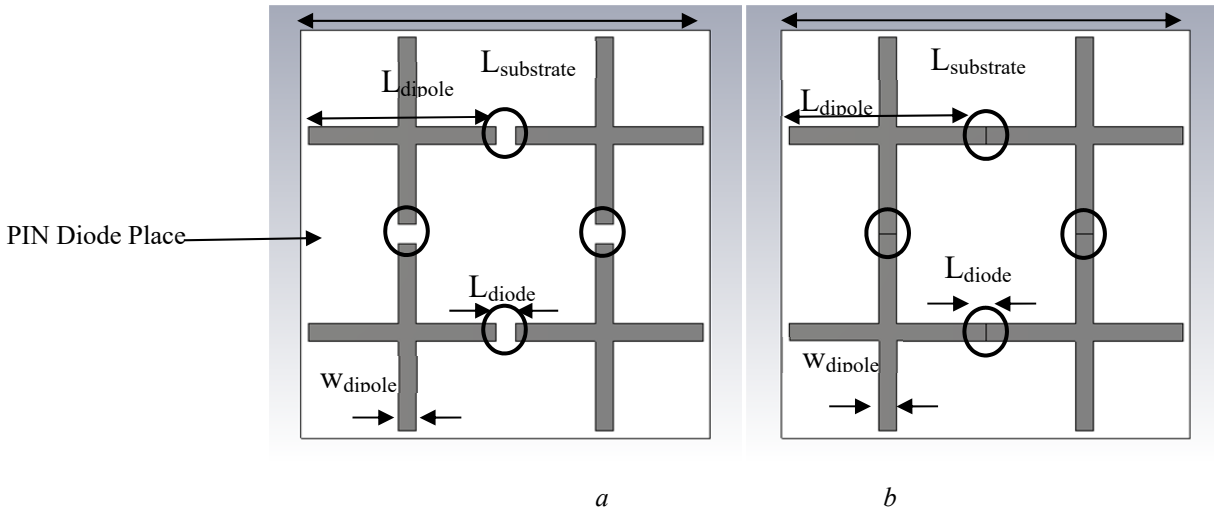


Fig. 6. Proposed unit cell
a Cross dipole
b Hash

For the following steps 2, 3 and 4 in the flowchart, a freestanding FSS was simulated using the full-wave commercial software CST Microwave Studio and its S21 values were stored. Using the LC series and LC parallel circuit models to represent the cross dipole and the hash states of the RFSS, respectively, the LC values were extracted using equations (2), (3) and (4). Equation (2) was derived from the relationship between the ABCD matrix of the discrete circuit and S parameters. Equation (3) was derived by circuit analysis.

$$Z_{FSS} = \frac{Z_0 S_{21}}{2(1 - S_{21})} \quad (2)$$

$$Z_{FSS} = \frac{j(\omega^2 L_0 C_0 - 1)}{\omega C_0} \quad (3)$$

$$C_0 = \frac{1}{\omega_0^2 L_0} \quad (4)$$

Z_0 is the impedance of air, Z_{FSS} is the impedance of the FSS and ω_0 is the resonance frequency. The discrete values of the equivalent circuit model for these structures are shown in Table 2 (step 4).

Following step 5, the capacitance of the discrete elements is adjusted according to the dielectric used:

$$C = C_0 \varepsilon_{eff} \quad (5)$$

Where,

$$\varepsilon_{eff} = \varepsilon_r + (\varepsilon_r - 1) \left(\frac{-1}{\text{Exp}(x)^N} \right), \quad (6)$$

$$x = 10d / D_0, \quad (7)$$

C_0 is the initial capacitance, d is the thickness of the dielectric, D_0 is the periodicity (length of the unit cell), ε_r is the relative permittivity and N is an exponential factor that takes into account the slope of the curve [11]. This parameter varies for different cell shapes as a function of the unit-cell filling factor. For the hash and cross dipole unit cell, the optimal value is $N = 2.2$. The dielectric substrate used is RT / Duroid 5880, which has a dielectric constant of 2.2, and a thickness of 0.65 mm. The discrete values of the equivalent circuit model for these structures are shown in Table 2 (step 5). When a dielectric is added to the

ideal freestanding structure, the resonant frequency is shifted. To adjust the resonant frequency to $f_0=12.5$ GHz, the periodicity must be changed in inverse proportion to the frequency.

The resulting dimensions for this step 6 are shown in table 1, and values of the equivalent circuit model are shown in table 2. Fig. 7 presents the final equivalent circuit models used for the proposed structures. Fig. 7 (a) models a pole at 12.04 GHz for the cross dipole, i.e. the point with maximum reflection. Fig. 7 (b) models a zero at 10.64GHz for the hash, i.e. the point with maximum transmission.

From the calculations obtained from step 6, the fabrication of the RFSS is done using a PCB Prototype Machine, the fabricated circuits that correspond to the two states of the RFSS are shown in figure 8.

Table 1 Dimensions (mm) for the initial and final step

Step	$L_{\text{substrate}}$	L_{dipole}	W_{dipole}	L_{diode}
1	26.6	12	1	1.3
6	20.8	9.4	0.8	1

Table 2 Equivalent circuit model, discrete elements

Step	Cross Dipole – LC series		Hash – LC Parallel	
	L (nH)	C (fF)	L (nH)	C (fF)
4	10.24	17.06	2.00	112.00
5	10.24	25.60	2.00	150.00
6	8.00	20.00	1.56	117.00

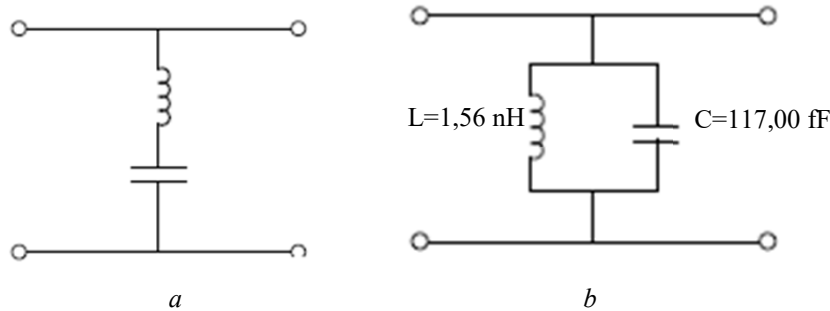


Fig. 7. Final equivalent circuit model

a Cross dipole

b Hash

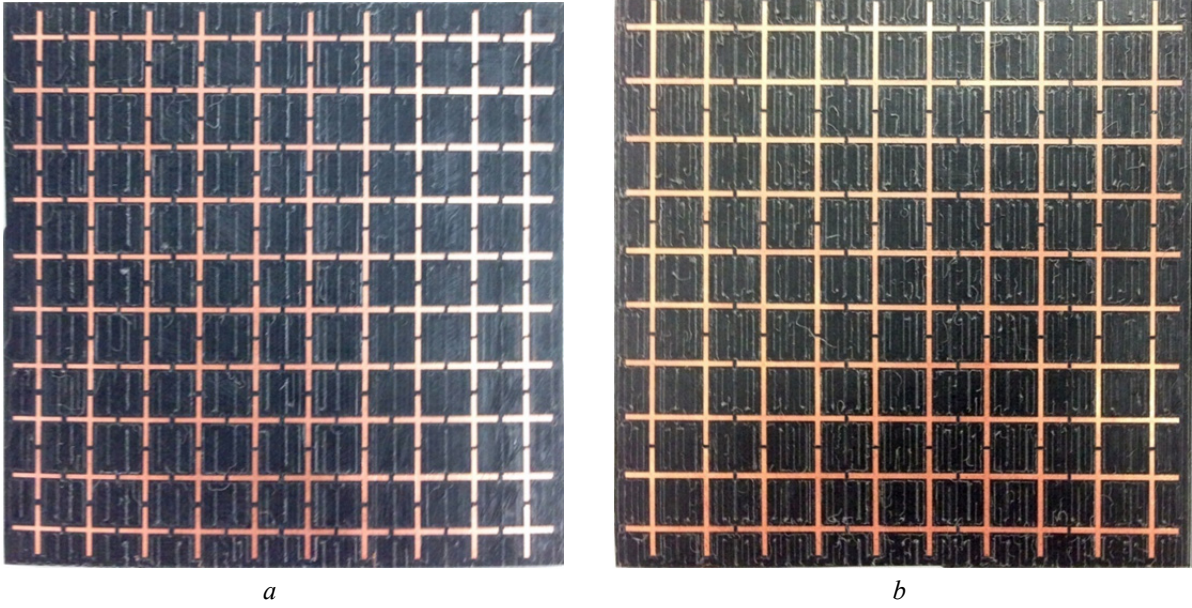
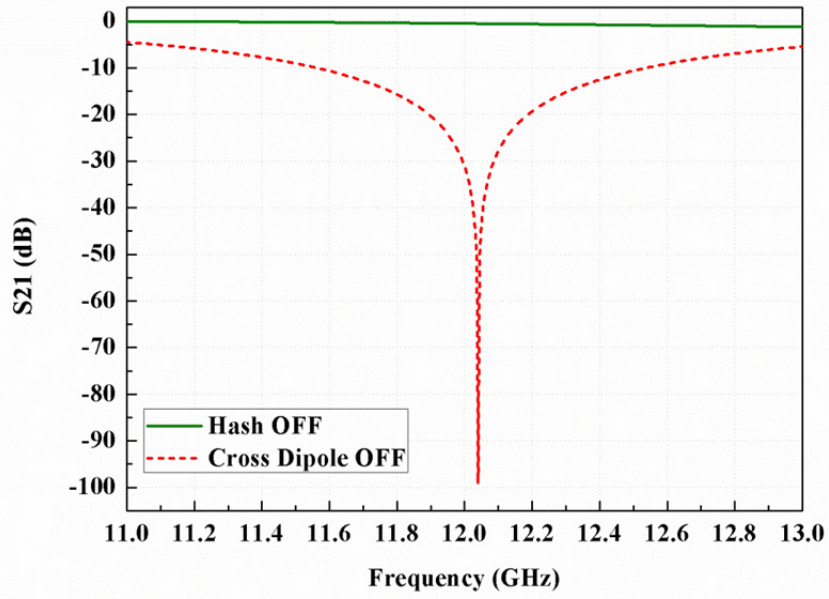


Fig. 8. FSS manufactured
a Cross dipole
b Hash

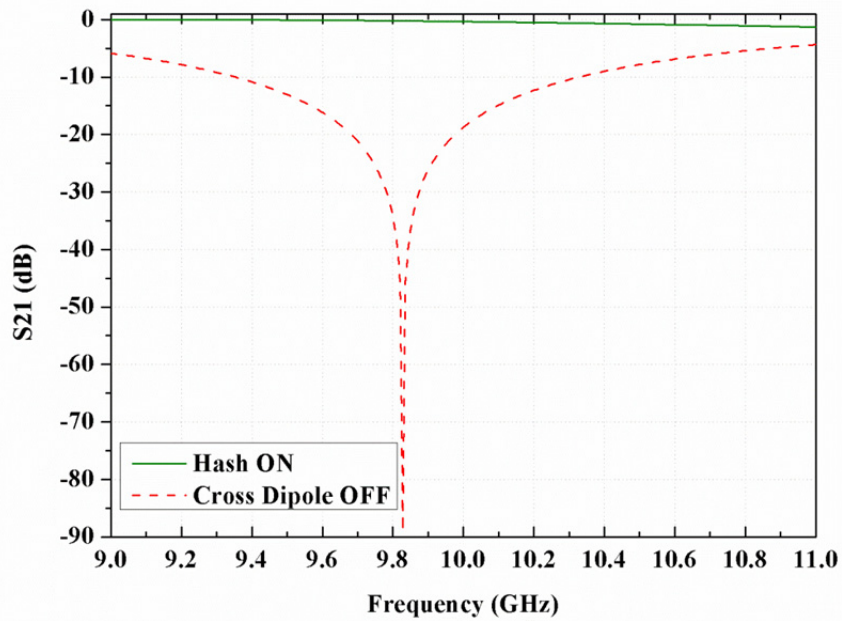
6. Results and Discussions

Initially the freestanding FSS cross dipole was designed to resonate at $f_0=12.5$ GHz, but observing the equivalent circuit's simulation results presented in Fig. 9 (a), the resonance frequency was $f_0'=12.04$ GHz. This shift in frequency is because the resonance frequency does not depend only on Eq. (1), but also depends on other factors such as periodicity of the FSS. Eq. (1) is only an estimate to find the approximate resonance frequency. The FSS on hash state has transmission characteristics with maximum at $f_0'=10.64$ GHz while on cross dipole state, the FSS has reflection characteristics with maximum at $f_0'=12.04$ GHz.

Fig. 9 (b) shows the simulation of the equivalent circuit that represents the FSS using the dielectric RT/Duroid 5880. There is a resonance frequency shift due to the new capacitance value given by Eq. (5).



a



b

Fig. 9. *S₂₁ parameters*

a Equivalent circuit model response for the FSS without dielectric at cross dipole and hash states with resonant frequency $f_0' = 12.04$ GHz

b Equivalent circuit model response for the FSS with dielectric RT/Duroid 5880 at cross dipole and hash states

Fig. 10 shows the simulation of the equivalent circuit that represents the final FSS with the desired resonance frequency near 12.5 GHz. From Fig. 10 at the hash state, the FSS behaves as a few transparent structure, and at the cross dipole state, the FSS behaves as a reflect structure.

Various methods can be used to measure the reflection and transmission properties of an FSS structure. Usually horns are placed on both sides of the FSS structure, used for transmission and reception of signals. The horn antennas can be configured for vertical and horizontal polarization, thus TE and TM transmission characteristics can be measured. First, with this configuration, it is possible to measure the reflection caused by the FSS, however erroneous data may be obtained due to the strong diffraction caused by the edges of the measured device. These diffractions may be due to the dimensions of the FSS which generally are significantly smaller than the beam width of horns [12].

Device measurements were made using a vector network analyser from Agilent Technologies model N5230A at the IFPB's laboratory, as shown in Figure 11. With this equipment it is possible to measure the modulus and phase of the scattering parameters directly in the range from 300 kHz to 20 GHz. Figure 12 (a) shows the experimental result for the RFSS. Still from the Figure 12 (a), at cross dipole state, the FSS behaves as a reflect structure with minimum $S_{21} = -38.16$ (dB) at $f = 12.61$ GHz, and at the same frequency, at hash state, the FSS transmits with $S_{21} = -2.91$ dB.

Figure 12 (b) and (c) show the result comparison between the equivalent circuit model, CST microwave simulation and measurements. Figure 12 (b) shows the transmission at the cross dipole state. The maximum reflections are -52.1 dB at 12.58 GHz, -38.16 dB at 12.61 GHz and -51.3 dB dB at 12.58 GHz, respectively obtained by simulations, measurements and equivalent model. Figure 12 (c) shows the transmission obtained for the hash state. The insertion losses for that same frequencies are -0.9 dB at 12.58 GHz, -2.91 dB at 12.61 GHz and -0.02 dB dB at 12.58 GHz, respectively obtained by simulations, measurements and equivalent model. A insertion loss value of $S_{21} = -2.91$ dB could be better, however, it may be considered an acceptable value considering an open bench structure without absorber and anechoic chamber. The difference between the insertion loss comparing the hash and cross dipole state is the most important aspect as far as applications are concerned. On hash state is -2.91 dB and cross dipole state is -38.16 dB.

Table 3 shows the PIN diode lumped element equivalent circuits used for the simulations. These circuits are based on the commercial MA4AGP907 diode and corresponds to a series RL circuit for forward bias, and a parallel RC circuit for reverse bias. To become the simulation results more real, these PIN diode model are used. The simulations results are shown in Fig. 12 (d). There is a shift of 0.6 GHz

when the model is included. This shift is probably related to the Diode isolation. The higher the isolation the smaller the shift.

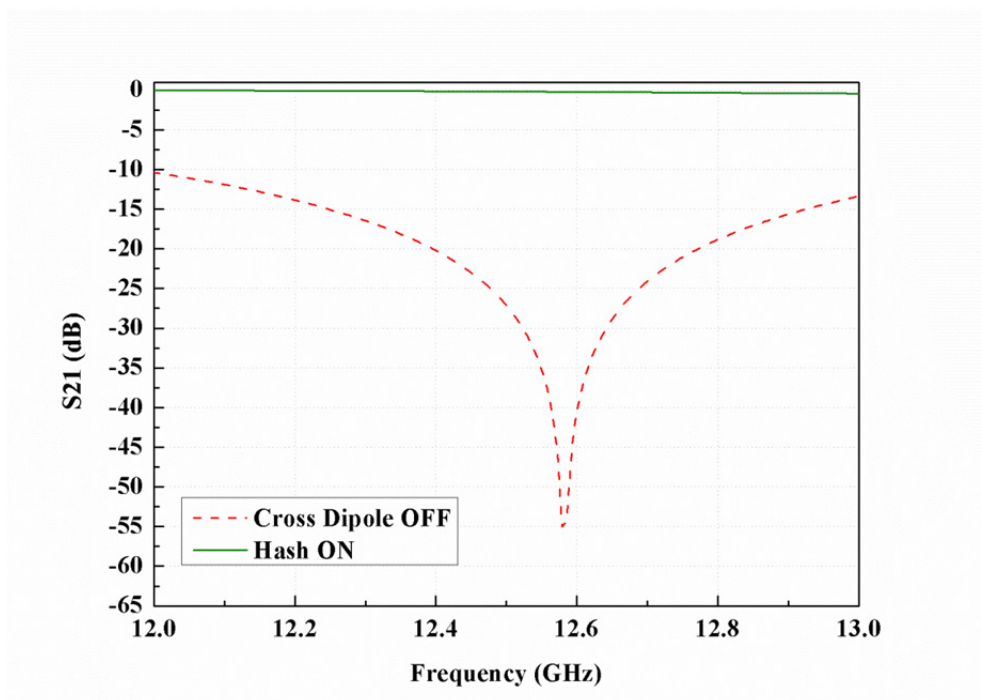


Fig. 10. Equivalent circuit model response for the FSS operating at 12.58 GHz at cross dipole and hash states

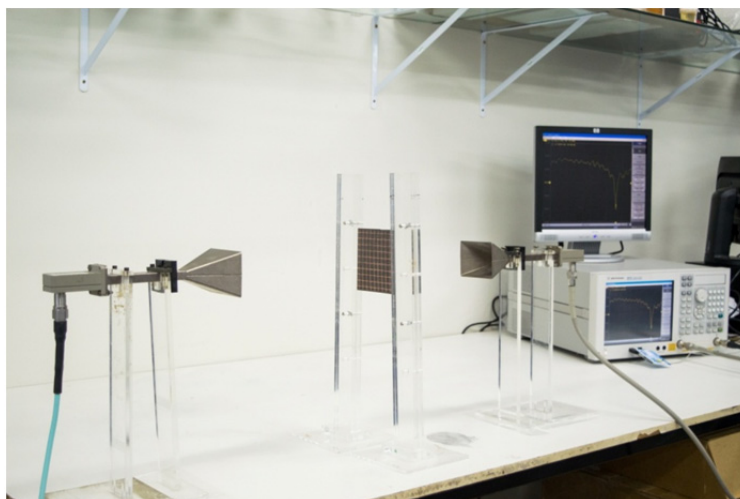
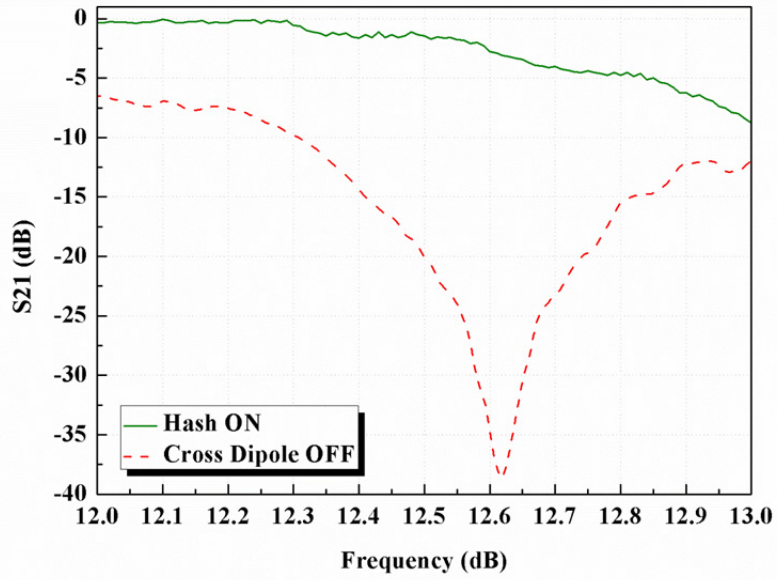
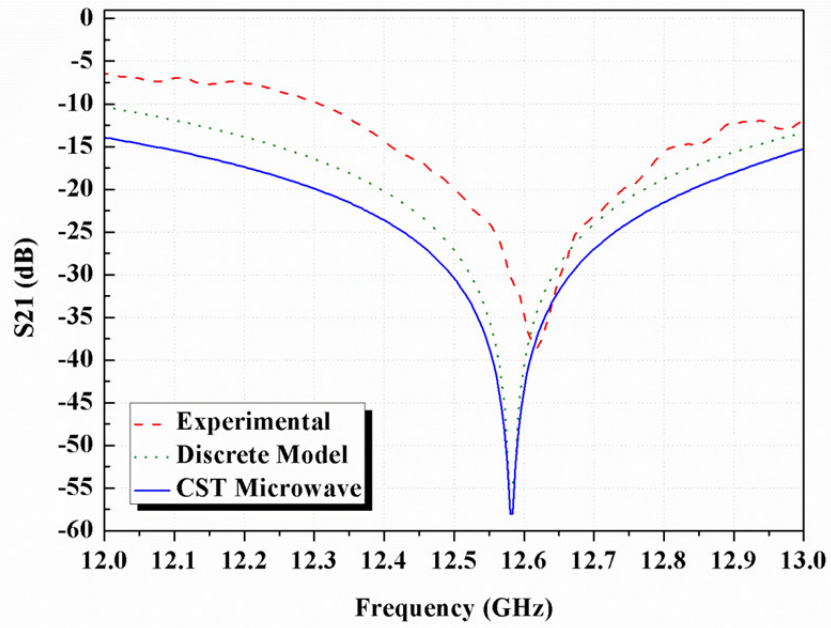


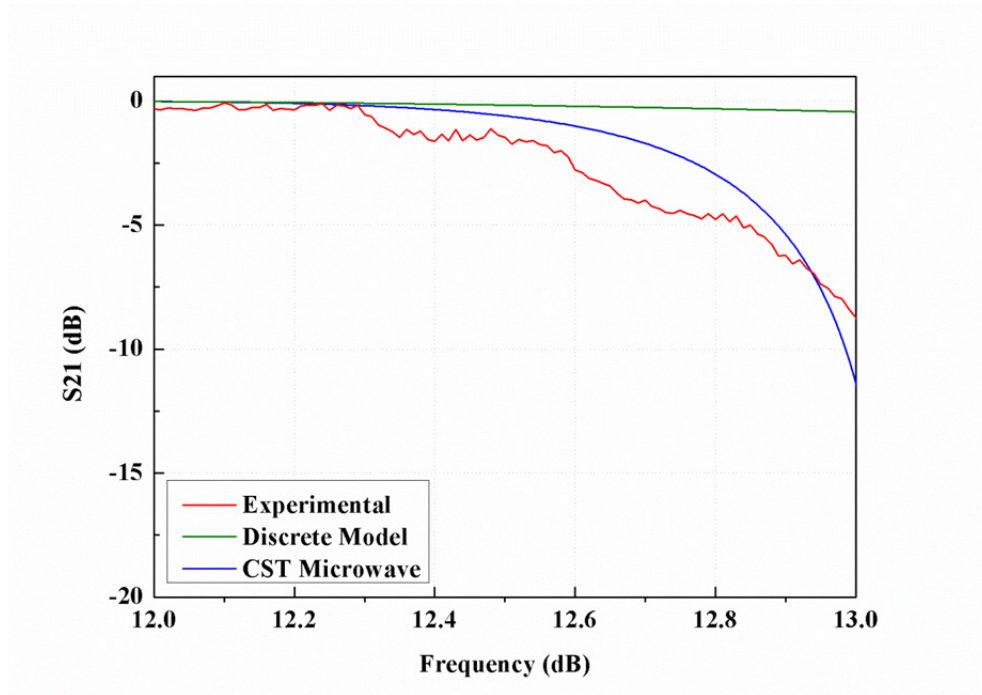
Fig. 11. Measurement arrangement of the FSS with horn antennas and the Agilent vector network analyser.



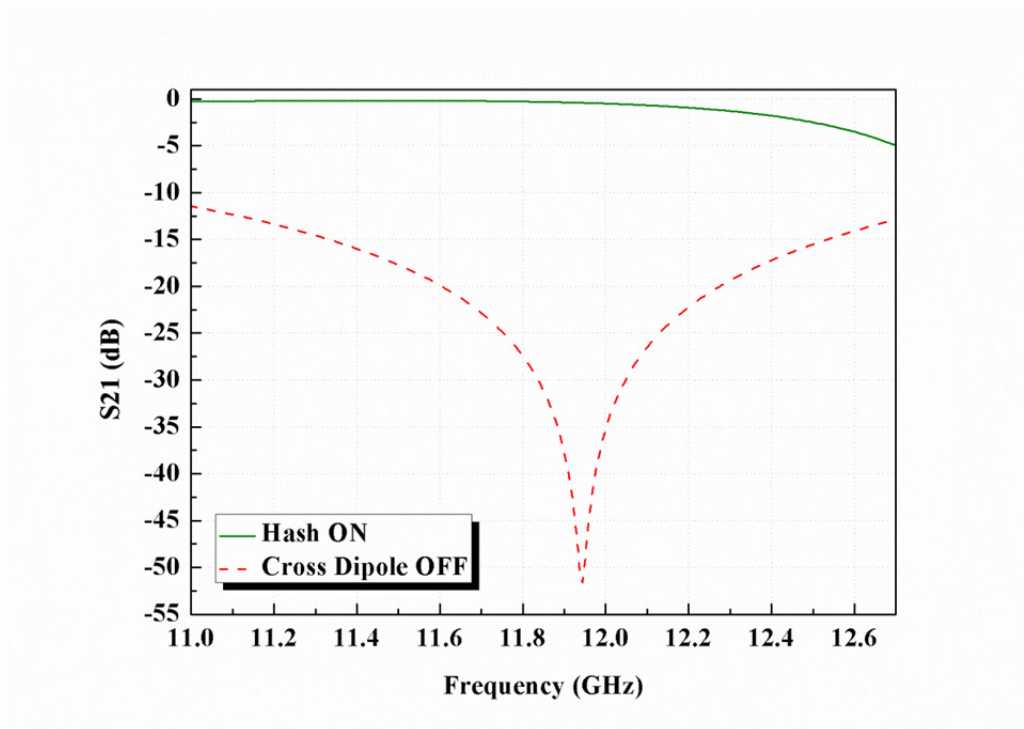
a



b



c



d

Fig. 12. *S21* parameters


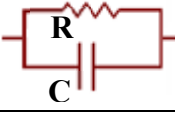
a Experimental results for the FSS operating at 12.61 GHz for cross dipole and hash states

b Comparison among results obtained by CST simulations, discrete model and experimental results for the cross dipole state

c Comparison among results obtained by CST simulations, discrete model and experimental results for the hash state

d Simulation results for the FSS with PIN diode modelling

Table 3 PIN diode equivalent circuits (MA4AGP907)

Forward bias (ON-State)		Reverse bias (OFF-State)	
			
R	L	R	C
4.5 Ω	0.6 nH	39 Ω	0.15 pF

7. Conclusions

The proposed RFSS performs as predicted by both simulations and calculations, verified through experimental results. The RFSS transmits with some losses at the hash state, and at the cross dipole state, the FSS behaves as a reflect structure. This feature finds its application in adaptive and RFID antennas.

The equivalent series LC circuit model for the cross dipole and the parallel LC model for the hash represent adequately the two states of the RFSS. These discrete models of the structures allow a flexible RFSS design approach. In addition, the method used to design and analyse the RFSS is efficient, fast and accurate enough to predict the performance of these surfaces.

Further work includes replacing the ideal short and open circuits used to demonstrate the RFSS structure in this paper for surface mount PIN diodes with their respective bias circuits. The next steps of this work also include the use of genetic algorithms to optimize the design. After the optimization of these structures, they can be used for applications in adaptive and RFID antennas.

8. Acknowledgments

This work was financed by Brazilian Science Agencies CNPq and CAPES. Part of this work has been supported by the Generalitat de Catalunya under grant 2014 SGR 1551.

9. References

- [1] D. Rittenhouse, "An optical problem, proposed by Mr. Hopkinson, and solved by Mr. Rittenhouse". *Trans. Amer. Phil. SOC.*, vol. 2, pp. 201-206, 1786.
- [2] D. B. Brito, "Metamaterial inspired improved antennas and circuits", UFRN Graduate Engineering in Electrical and Computer Engineering and Telecom Graduate Program in Electronics and Telecommunications: D. Sc. Dissertation, 2010.

- [3] T. Chang, R. Langley e E. Parker, “An Active Square Loop Frequency Selective Surface”. *Microwave and Guided Wave Letters*, IEEE, vol. 3, no. 10, pp. 387-388, October 1993.
- [4] J. Yuan, S. Liu, X. Kong e H. Yang, “A reconfigurable frequency selective surface for tuning multi-band frequency response separately”. *Antennas & Propagation (ISAP), Proceedings of the International Symposium on*, Vol. 02, pp. 1288 – 1290, October 2013.
- [5] G. Kiani, K. Esselle, A. Weily e K. Ford, “Active Frequency Selective Surface Using PIN Diodes,” *Antennas and Propagation Society International Symposium, IEEE*, pp. 4525 - 4528, June 2007.
- [6] J. Huang, T.-K. Wu e S.-W. Lee, “Tri-band frequency selective surface with circular ring elements”. *Antennas and Propagation, IEEE Transactions on*, pp. vol.42, no. 2, pp. 166-175, February 1994.
- [7] R. Mittra, C. Chan e T. Cwik, “Techniques for analysing frequency selective surfaces-a review”. *Proceedings of the IEEE*, pp. vol. 76, no.12, pp. 1593-1615, December 1988.
- [8] J. Bossard, D. Werner, T. Mayer e R. P. Drupp, “A novel design methodology for reconfigurable frequency selective surfaces using genetic algorithms”. *Antennas and Propagation, IEEE Transactions on*, vol. 53, no.4, pp. 1390-1400, April 2005.
- [9] B. A. Munk, “Frequency-selective surfaces: theory and design”, New York: John Wiley & Sons, 2000.
- [10] J. Bossard, D. Werner, T. Mayer e R. P. Drupp, “A novel design methodology for reconfigurable frequency selective surfaces using genetic algorithms”. *Antennas and Propagation, IEEE Transactions on*, vol. 53, no. 4, pp. 1390-1400, April 2005.
- [11] F. Costa, “Efficient analysis of frequency-selective surfaces by a simple equivalent-circuit model”. *IEEE Antennas and Propagation Magazine*, vol. 54, no. 4, pp. 35–48, 2012.
- [12] Y. Li, L. Li, Y. Zhang and C. Zhao, "Design and Synthesis of Multilayer Frequency Selective Surface Based on Antenna-Filter-Antenna Using Minkowski Fractal Structures," in *IEEE Transactions on Antennas and Propagation*, vol. 63, no. 1, pp. 133-141, January 2015.